

## LEPTON DECAY CHANNELS OF EGRET GLUINOS AT THE LHC

*V. A. Bednyakov<sup>a</sup>, J. A. Budagov<sup>a</sup>, A. V. Gladyshev<sup>a</sup>, D. I. Kazakov<sup>a</sup>,  
E. V. Khramov<sup>a</sup>, D. I. Khubua<sup>a, b</sup>*

<sup>a</sup> Joint Institute for Nuclear Research, Dubna

<sup>b</sup> Institute of High Energy Physics and Informatics, Tbilisi State University, Tbilisi, Georgia

Prospects for observation of a SUSY-like signal from two gluinos  $\tilde{g}\tilde{g}$  are investigated within a certain region of the mSUGRA parameter space, where the cross section of the two gluino production in  $pp$  collisions at the LHC ( $\sqrt{s} = 14$  TeV) via gluon–gluon fusion,  $gg \rightarrow \tilde{g}\tilde{g}$ , is estimated at a rather high level of 17.3 pb. In this so-called EGRET region the lightest stable neutralinos can serve as cold dark matter particles and can naturally explain the excess of diffuse galactic gamma rays observed by the EGRET space apparatus. The  $\tilde{g}\tilde{g}$ -event selection relies on a very clear signature when decay products of each gluino contain one  $b$ –anti- $b$  pair, one or two lepton–antilepton pair(s) and a neutralino. Rather high transverse missing energy carried away by the two neutralinos is an essential signature of the events and also allows the relevant Standard Model background to be reduced significantly. In particular, it was found that the clear signatures of the selected processes demonstrate good prospects for discovery of the EGRET gluinos at the LHC. Furthermore, these signatures allow one to distinguish different mSUGRA parameters  $m_{1/2}$  within the EGRET region.

Исследована возможность наблюдения на LHC сигнала от рождения двух SUSY-глюино,  $\tilde{g}\tilde{g}$ , характеристики которых определяются так называемой EGRET-областью пространства параметров mSUGRA. В этой области сечение образования пары глюино (посредством глюон–глюонного слияния  $gg \rightarrow \tilde{g}\tilde{g}$ ) в  $pp$ -столкновениях на LHC ( $\sqrt{s} = 14$  ТэВ) достигает достаточно большой величины в 17,3 пб. Кроме того, в этой EGRET-области легчайшие и стабильные нейтралино являются частицами холодной темной материи и естественным образом объясняют избыток рассеянного галактического гамма-излучения, зарегистрированного космическим аппаратом EGRET. Выделение из фона на LHC таких  $\tilde{g}\tilde{g}$ -событий опирается на очень отчетливую их сигнатуру распада, когда продуктами распада каждого из глюино являются одна пара  $b$ –анти- $b$ -кварков, одна или две пары заряженных лептон–анти-лептонов и одно нейтралино. Достаточно большая величина недостающей поперечной энергии, уносимой двумя стабильными нейтралино, — важная характеристика этих событий, позволяющая в очень сильной форме подавить фоновые события, источником которых являются процессы в рамках Стандартной модели. В частности, показано, что обнаруженные отчетливые сигнатуры рассмотренных SUSY-процессов дают реальную возможность регистрации указанных выше EGRET-глюино при энергиях LHC. Более того, характеристики рассмотренных событий позволят также определить наиболее предпочтительное в EGRET-области значение mSUGRA параметра  $m_{1/2}$ .

PACS: 12.60Jv, 14.65Ha

## INTRODUCTION

Search for and discovery of Higgs boson(s) and supersymmetric (SUSY) particles are nowadays the two most fundamental goals of the Large Hadron Collider (LHC) which is created at CERN (Geneva) by huge international collaboration. Very soon the LHC is planned to face with ATLAS and CMS detectors the first proton–proton collisions at the highest accelerator energies. Due to unknown masses the discovery of the SUSY particles (as well as Higgs bosons) is a very strong challenge for the modern particle and accelerator physics. This is why one has to look for and carefully study any possible SUSY particle signatures which could allow one to prove the expected SUSY discovery.

The minimal SUSY version of the Standard Model (MSSM) with universal soft supersymmetry breaking terms induced by supergravity (mSUGRA) [1] has a minimal set of free parameters:  $m_0$ ,  $m_{1/2}$ ,  $\text{sign } \mu$ ,  $A_0$ ,  $\tan \beta = v_2/v_1$ , where  $m_0$  and  $m_{1/2}$  are common mass parameters for the scalar and spinor superpartners at the unification scale, respectively,  $\mu$  is the Higgs mixing parameter,  $A_0$  is the trilinear soft supersymmetry breaking parameter, and  $\tan \beta$  is the ratio of vacuum expectation values of two Higgs fields. The allowed values of these parameters are restricted by theoretical and experimental constraints, as well as by WMAP astrophysical data [2].

In supersymmetric models with conserved  $R$  parity, the superpartners of ordinary particles can be created only in pairs, which leads to the existence of the stable lightest supersymmetric particle (LSP). Usually it is the lightest neutralino, being an electrically neutral, massive and weakly interactive particle. In the mSUGRA the masses of the superpartners at some energy scale can be calculated by solving renormalization group equations with the parameters mentioned above being initial conditions at the unification scale (except  $\tan \beta$ ).

In the region with large scalar mass parameters  $m_0$  and small fermion mass parameters  $m_{1/2}$  (Fig. 1), the LSP properties are consistent with the observed relic density; i.e., the LSP can serve as cold dark matter particle; furthermore, the LSP can naturally explain the excess of diffuse galactic gamma rays observed by EGRET [3], as well as the DAMA evidence

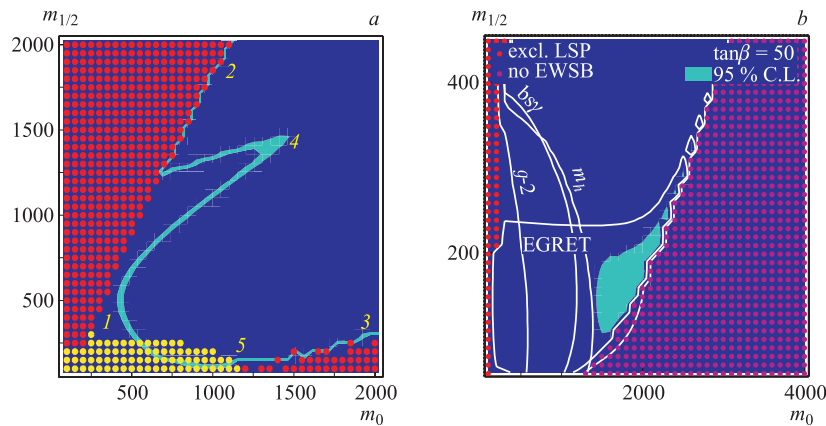


Fig. 1. *a*) The mSUGRA  $m_0 - m_{1/2}$  parameter space. Light line in the middle corresponds to the region consistent with WMAP data. The EGRET region is marked with 5. *b*) The light shaded area is the enlarged region preferred by EGRET data for  $\tan \beta = 50$ ,  $\mu > 0$  and  $A_0 = 0$ . The excluded regions are indicated by the dots

for direct dark matter detection via annual modulation [4, 5]. The typical set of the EGRET region parameters (used in the analysis) is the following (Fig. 1):

$$m_0 = 1400 \text{ GeV}, m_{1/2} = 180 \text{ GeV}, \text{sign } \mu = +1, A_0 = 0, \tan \beta = 50. \quad (1)$$

It appears to be very interesting phenomenologically because of the mass splitting between the light weak-interacting gauginos and the heavy sleptons and strong-interacting squarks. The cross sections for the chargino and neutralino production at the LHC are rather large and are comparable with the cross sections of the squark and gluino production. The latter, being enhanced by strong interaction, remains suppressed by heavy masses of the squarks. Therefore, in the EGRET region the leptonic processes with neutralinos and charginos are not suppressed and might give clear leptonic signature for SUSY in the upcoming LHC experiments [6]. Furthermore, detection of SUSY-like signal(s) which correspond to the EGRET point would be a strong indication both of the supersymmetry and of solution of the dark matter problem.

The parameters (1) were used as input for the ISAJET code [7] which calculated the superparticle spectrum at the EGRET region. Afterwards, this mass spectrum was used by the PYTHIA generator [8] for the event generation. The superparticle mass spectrum and the cross sections of different SUSY processes depend on the chosen parameters of mSUGRA. The common property of the SUSY-like processes with conserved  $R$  parity is undetectable LSP(s) in the final state. These LSPs are rather heavy and thus take away quite large (and undetectable) transverse momentum. The condition for choosing the certain SUSY process (or observable) was not only its large cross section but also a peculiar signature which allows one to separate it from different Standard Model background events. Very clear signature for detection of these so-called EGRET gluinos was found for the first time in our previous paper [9]. The parton-level process of pair gluino,  $\tilde{g}$ , production (via gluon–gluon fusion) and subsequent gluino decays can be presented as the following chain (given below for one of these gluinos):

$$\begin{aligned} gg \rightarrow g^* \rightarrow \tilde{g}\tilde{g} \\ \downarrow \\ \bar{b} + b + \tilde{\chi}_2^0 \\ \downarrow \\ l^-(q) + l^+(\bar{q}) + \tilde{\chi}_1^0. \end{aligned} \quad (2)$$

Each gluino in the chain (2) first decays into the  $b\bar{b}$  pair and the second neutralino  $\tilde{\chi}_2^0$ , afterwards the  $\tilde{\chi}_2^0$  decays into the lepton- ( $\mu^+\mu^-$ , or  $e^+e^-$ ) or light-quark- ( $q\bar{q}$ ,  $q = u, d, c, s$ ) pair and the LSP neutralino  $\tilde{\chi}_1^0$ . In both three-particle decays (in the EGRET region) the intermediate vector neutral bosons ( $Z \rightarrow b\bar{b}$  and  $Z \rightarrow l^+l^-$ ) are far off shell. In accordance with [6] the subdominant contributions of the gluino decay into  $\tilde{\chi}_{1,3,4}^0$  were not considered. From the chain (2) one can distinguish three types of final states of the two gluino production.

The first so-called «dilepton» channel of  $\tilde{g}\tilde{g}$ -pair decay contains four  $b$  jets, two opposite-sign (OS) charged lepton pairs and two LSP neutralinos  $\tilde{\chi}_1^0$  in the final state (Fig. 2):

$$pp \rightarrow \tilde{g}\tilde{g} + X \rightarrow 4b_{\text{jets}} + 2l^+l^- + 2\tilde{\chi}_1^0 + X. \quad (3)$$

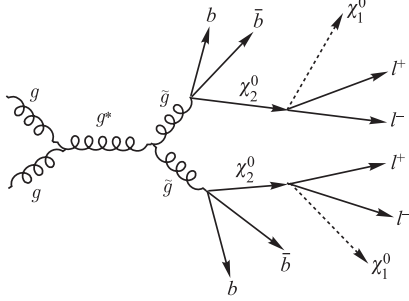


Fig. 2. The «dilepton» decay channel of  $\tilde{g}\tilde{g}$  pair with four  $b$  jets (or four secondary vertices) and two opposite-sign charged lepton pairs. The two LSP neutralinos,  $\tilde{\chi}_1^0$ , escape their detection

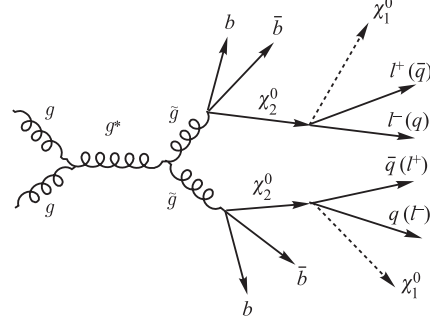


Fig. 3. The «lepton plus jets» and «multijet» decay channels of  $\tilde{g}\tilde{g}$  pair with four  $b$  jets, one opposite-sign charged lepton pair and one light-quark pair

Here  $X$  denotes all other particles originated from initial protons. The second, «lepton plus jets» (or «lepton + jets») gluino pair decay channel has four  $b$  jets and two  $\tilde{\chi}_1^0$ , one OS charged lepton pair and one light-quarks pair (Fig. 3) in the final state:

$$pp \rightarrow \tilde{g}\tilde{g} + X \rightarrow 4b_{\text{jets}} + l^+l^- + q\bar{q}_{\text{jets}} + 2\tilde{\chi}_1^0 + X. \quad (4)$$

Finally, the third, «multijet» channel of  $\tilde{g}\tilde{g}$ -pair decay contains again four  $b$  jets and two  $\tilde{\chi}_1^0$ , but now two light-quarks pairs without any charged lepton in the final state (see also Fig. 3).

In what follows the first two *leptonic*  $\tilde{g}\tilde{g}$ -pair decay channels (dilepton and lepton + jets) are studied at the generation level and the optimal selection criteria for them are elaborated (Sec. 1). The background investigations are carried out in Sec. 2. Conclusions about possibility for these gluinos observation at the LHC energies, as well as the «true» EGRET point localization, are formulated in the final section.

## 1. RECONSTRUCTION OF EVENTS

To single out and understand the main features (signatures) of the selected process (2), one should first of all study it at the generation level, when all hard and soft subprocesses are under clear control.

In this section we at first consider the «dilepton» channel of the  $\tilde{g}\tilde{g}$ -pair decay (see Fig. 2 and Eq. (3)). Due to the fact that the PYTHIA branching ratios of the  $\tilde{\chi}_2^0$  decay into  $\tilde{\chi}_1^0$  via  $\mu^+\mu^-$  and  $e^+e^-$  pair are very similar:

$$\text{Br}(\tilde{\chi}_2^0 \rightarrow \tilde{\chi}_1^0 e^+e^-) \approx \text{Br}(\tilde{\chi}_2^0 \rightarrow \tilde{\chi}_1^0 \mu^+\mu^-) \sim 3.3\%,$$

the dilepton  $\tilde{g}\tilde{g}$ -pair decay channel has about 25% of events with two OS charged electron pairs, about 25% of events with two OS charged muon pairs and about 50% with one OS electron and one OS muon pairs. There are four  $b$ -type quarks (two  $b$  and two  $\bar{b}$  quarks) in the dilepton event. The lifetime of the gluino is very small; therefore, all these  $b$  quarks are created practically in the primary vertex of the  $pp$  collision (see, for illustration, Fig. 4).

Afterwards they almost immediately hadronize (at a distance from the primary vertex about  $10^{-13}$  cm) and produce the so-called  $b$  jets which can contain, in particular, relatively long-lived  $B$  hadrons.

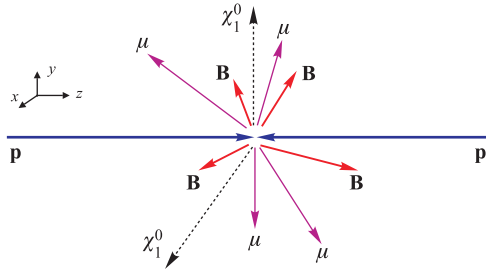


Fig. 4. Scheme of the «dilepton» process. Here  $\mathbf{p}$ ,  $\mathbf{B}$  and  $\mu$  denote initial-state proton, final-state muon and  $B$  meson, respectively. Escaping LSP is given by  $\tilde{\chi}_1^0$

The  $B$  hadron can fly away from the primary vertex and decaying can produce the secondary vertex at a measurable distance of 1–10 mm from the primary vertex. Therefore, all two-gluino induced events (dilepton, lepton + jets and multijets, see (2)) could, in general, have four secondary vertices, which allow on-line background reduction (at the trigger level).

At the LHC the cross section of the considered gluon–gluon fusion gluino production via  $pp(gg) \rightarrow g^* \rightarrow \tilde{g}\tilde{g} + X$  is quite large [6]. It depends on the parton distribution functions (PDF) for the proton and their dependence on the transfer momentum  $Q^2$ . The PDF model CTEQ6L1 with  $Q_{\min}^2 = 1.69$  GeV [10] gives about 17.3 pb for the cross section for this process. The variation of the total cross section of the dilepton process with different PDF models is shown in Table 1. One can conclude from the table that the total cross section

could, in general, have four secondary vertices, which allow on-line background reduction (at the trigger level).

Table 1. Cross sections of the full dilepton process  $pp \rightarrow \tilde{g}\tilde{g} \rightarrow (b\bar{b}\tilde{\chi}_2^0)(b\bar{b}\tilde{\chi}_2^0) \rightarrow (b\bar{b}\tilde{\chi}_1^0\mu^+\mu^-)(b\bar{b}\tilde{\chi}_1^0\mu^+\mu^-)$  at  $\sqrt{14}$  TeV as function of the PDF model

PDF Model and Ref.	$\sigma(pp \rightarrow \tilde{g}\tilde{g})\text{Br}(\tilde{g}\tilde{g} \rightarrow 2(b\bar{b}\tilde{\chi}_1^0\mu^+\mu^-))$ , fb
CTEQ6L1 [10]	0.599
MRST_2001_nlo [12]	0.851
MRST_2004_nnlo [13]	0.991
Fermi_2002_1000 [14]	0.723
Alekhin_1000 [15]	0.877
Botje_1000 [16]	0.540

(and therefore final number of expected events) of the dilepton two-gluino-decay channel has systematic uncertainties at a level of factor 2 due to different interpolations of different PDF models into the new energy region of the LHC. Perhaps, it is a right moment to stress that, to produce reliable expectations for some peculiar process, one better has to rely not on interpolations of PDF, but on their careful measurements in the energy region of interest.

To study peculiarities of the dilepton channel (3), some transverse momentum  $P_t$  distributions for both gluino decay products are calculated with PYTHIA event generator [8]. In Fig. 1 these distributions for  $b$ -quark pair (forming two  $b$  jets), for OS lepton pair and for the lightest neutralinos are depicted.

One can see that neutralinos take away quite high transverse momentum. It is worth noticing that in the real experiment one can measure only the transverse missing (undetected) energy of two neutralinos  $E_T^{\text{miss}}$ . Figure 6 shows the total transverse momentum of two neutralinos. It is clear that the careful reconstruction will allow one to detect such a high

loss in the total measure transverse energy. This is the first specific feature (signature) of the considered dilepton channel of  $\tilde{g}\tilde{g}$ -pair decay which can be used for signal-to-background separation.

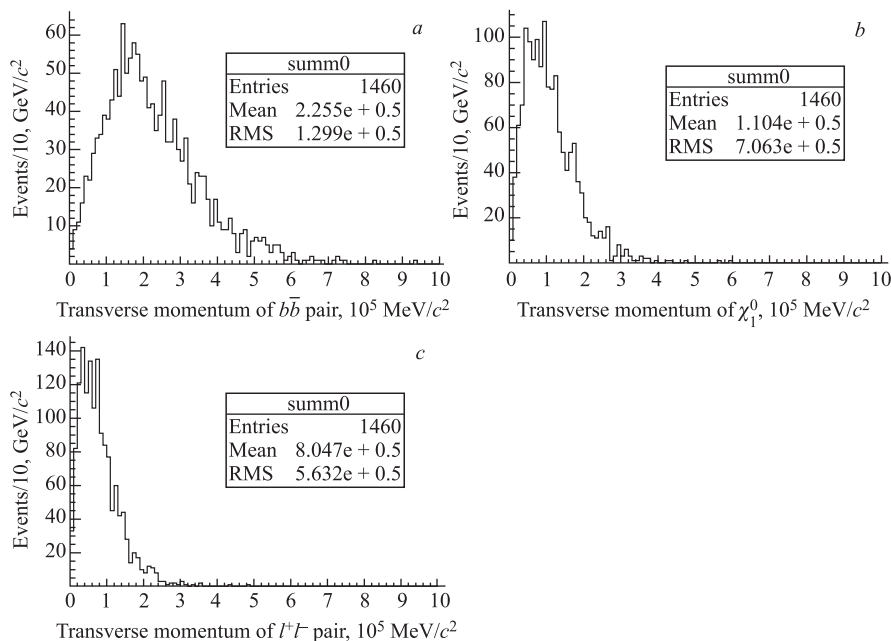


Fig. 5. Transverse momentum distributions for the products of both gluino decays in the dilepton channel. a) The total  $P_t$  for the  $b\bar{b}$  pairs; b)  $P_t$  for the lightest stable neutralinos  $\tilde{\chi}_1^0$  from the heavier neutralinos decay; c) the total  $P_t$  for the lepton pairs

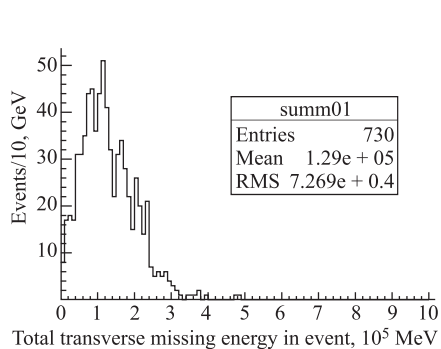


Fig. 6. Distribution on the total missing transverse momentum  $P_t$  of two neutralinos (defined as geometric sum  $E_T^{\text{miss}} = \sqrt{(p_x^1 + p_x^2)^2 + (p_y^1 + p_y^2)^2}$ , where  $p_x^{1,2}$  and  $p_y^{1,2}$  are  $x$  and  $y$  momentum components of the 1st and the 2nd LSPs, respectively)

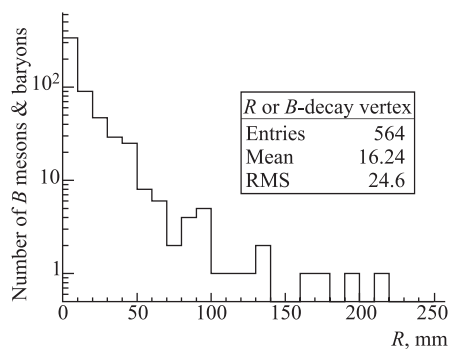


Fig. 7. The free path of the  $B$  hadrons created in the dilepton process (Fig.2) before their decay. The criterion for the event selection is that the free path is not less than  $100 \mu\text{m}$  for each of four  $B$  hadrons in the same event. 94% of events satisfy this condition

The second specific feature (signature) of the dilepton (as well as lepton+jets and multijets) channel of the  $\tilde{g}\tilde{g}$ -pair decay is the existence of four  $b$  jets in any event-candidate. Reliable identification of all these  $b$  jets (the so-called  $b$  tagging) and the careful reconstruction of their energies are extremely important for the study of the considered processes. The  $B$  hadrons with  $b$  quarks inside live rather long time and can move rather far away from the primary vertex (the cross point of initial proton beams). As a result, it allows one to observe a secondary vertex of  $B$ -hadron decay at a certain distance from the primary beams collision initial vertex. This secondary vertex allows one to tag hadronic jets from  $b$  quarks. Figure 7 shows the distribution of the free paths of the  $B$  hadrons provided all the four  $B$  hadrons have free paths more than  $100\ \mu\text{m}$  simultaneously. One can see that 94% of events satisfy this condition. On the basis of this free-path feature one can arrange criteria on the presence of a secondary vertex in the selected events and therefore one can create an (on-line) trigger for the effective  $b$ -jet separation.

All the distributions presented above were obtained for 730 events in the dilepton  $\tilde{g}\tilde{g}$ -pair decay channel. The number is expected after 3 years of the LHC running with total luminosity  $10^{34}\ \text{cm}^{-2}\cdot\text{s}^{-1}$  («high luminosity») for the EGRET region and CTEQ6L1 parton distribution functions. Other PYTHIA parameters were set to their default values, such as final-state radiation (FSR), initial-state radiation (ISR), multiple interactions are included [8].

Therefore, the generator level study of the dilepton decay channel of the two EGRET gluinos allows one to elaborate at least two clear signatures for the dilepton (3) and lepton + jets (4) processes. The common signatures are the large missing transverse energy, four  $b$  jets and OS lepton pairs.

**1.1. Endpoint Criteria in the Dilepton Channel.** From Fig.1 one can see that some variation of the SUSY parameters  $m_{1/2}$  and  $m_0$  around the EGRET point (1) are naturally allowed within the EGRET region. This variation results in alternation of the properties of SUSY particles (mainly masses), as well as expected dependence of cross sections of the «signal» processes (2) on these SUSY parameters (see, for example, Fig.8 from [6]). Careful investigation of these dependences in principle allows one to distinguish between different EGRET parameters  $m_{1/2}$  and  $m_0$  and determine from the future real experimental data some «true» SUSY parameters (the SUSY point) which would coherently describe all SUSY observables (at least in the EGRET region). Here we would like to stress *the general point* that such kind of coherent description of all SUSY observables is inevitable requirement to prove the experimental evidence of the SUSY observation.

On the way to solve this general problem, an investigation of sensitivity of the processes (2) to the mass parameter  $m_{1/2}$  was carried out. For integrated luminosity  $300\ \text{fb}^{-1}$  (three years at high luminosity of the LHC), special samples of the dilepton and lepton + jets events were generated in the EGRET region for three «subpoints» with  $m_{1/2} = 170, 180$  and  $190\ \text{GeV}$ , respectively (Table 2). All the other SUSY parameters in the region ( $m_0, A_0$ , etc.), were kept from (1).

In a hadron collider experiment, the masses of the SUSY particles can hardly be determined (kinematically) because of the missing energy carried away by the escaping LSP neutralino(s), as well as due to the lack of precise knowledge of the total initial energy of the colliding partons. One can however extract some information about SUSY particle masses by calculating the invariant masses of various combinations of particles from the cascade decays of SUSY particles until stable LSP(s). The inevitable presence of the LSP in the final state

of these cascade decays (SUSY  $R$ -parity is conserved) allows one to use in the analysis the so-called endpoint variable [19]. Below this endpoint variable is used to distinguish different subpoints in the EGRET region.

**Table 2. The total cross section of  $pp(gg) \rightarrow \tilde{g}\tilde{g} + X \rightarrow (\tilde{\chi}_2^0 b\bar{b})(\tilde{\chi}_1^0 b\bar{b}) + X$ , the numbers of events expected at the LHC with  $300 \text{ fb}^{-1}$ , the masses of two lightest neutralinos  $\tilde{\chi}_2^0$ ,  $\tilde{\chi}_1^0$  and these mass differences for  $m_{1/2} = 170, 180$  and  $190 \text{ GeV}$**

$m_{1/2}$	170 GeV	180 GeV	190 GeV
Total $pp \rightarrow \tilde{g}\tilde{g} + X$ cross section, fb	294.6	212.1	144
Number of dilepton events	1057 (3.4 fb)	681 (2.4 fb)	529 (1.7 fb)
Number of lepton+jets events	17040 (56.6 fb)	12339 (40.7 fb)	8104 (28.3 fb)
$m_{\tilde{\chi}_2^0}$ , GeV	114.53	125	133.91
$m_{\tilde{\chi}_1^0}$ , GeV	63.63	68	72.82
Expected $m_{\tilde{\chi}_2^0} - m_{\tilde{\chi}_1^0}$ , GeV	50.9	57	61.09

Considering the dilepton  $\tilde{g}\tilde{g}$ -pair decay channel (3), one requires the  $\tilde{\chi}_2^0$  decays into opposite charged lepton ( $e$  or  $\mu$ ) pair and the LSP  $\tilde{\chi}_1^0$ . Selection criteria for this decay mode (existence of four  $b$  jets and two OS lepton pairs) repeat signature in final state except the missing transverse energy due to the pair of  $\tilde{\chi}_1^0$ .

Thus, the invariant mass of this OS lepton pair,  $m_{ll}^{\text{expected}}$ , is always less than the difference between the masses of  $\tilde{\chi}_2^0$  and  $\tilde{\chi}_1^0$ ,

$$m_{ll}^{\text{expected}} \leq m_{\tilde{\chi}_2^0} - m_{\tilde{\chi}_1^0} \equiv M(\tilde{\chi}_2^0 - \tilde{\chi}_1^0), \quad (5)$$

where  $M(\tilde{\chi}_2^0 - \tilde{\chi}_1^0)$  is the endpoint variable. The distributions of the invariant masses of the opposite-sign charged lepton pairs,  $m_{ll}$ , obtained at the parton level are given in Fig. 8. All distributions show clear endpoint behavior.

It is quite easy to obtain distributions shown in Fig. 8 because after generation one has full information about development of every event. But at the experimental level this information will not be available. In the final state of the dilepton channel decay (3), except for four  $b$  jets and high missing energy (due to the loss of two  $\tilde{\chi}_1^0$ ), one has three combinations of two OS lepton pairs. There are two electron pairs or two muon pairs, or one electron pair and one muon pair. In the last case, when first  $\tilde{\chi}_2^0$  decays via muon pair and the second  $\tilde{\chi}_2^0$  decays via the electron pair, the right combinations of two leptons for the  $m_{ll}$  reconstruction is obvious. In the other two cases of the  $\tilde{\chi}_2^0$ -pair decay, there are two different combinations for two lepton pairs. The lepton pair combination is «truth» if both leptons are from the same  $\tilde{\chi}_2^0$  decay, and it is «false» if the two leptons are from different  $\tilde{\chi}_2^0$  decays. The distributions over the angle between the two leptons in the pair,  $\Delta\phi/\pi$ , for «truth» and «false» combinations of the opposite-sign charged leptons are calculated at the generation parton level for  $m_{1/2} = 180 \text{ GeV}$  and is given in Fig. 9. One can see that the «truth» combinations are, in general, closer to zero than the «false» combinations. The combinations of the two lepton pairs that give the smallest sum ( $\Delta\phi_1 + \Delta\phi_2$ ) are considered as a «truth» two lepton-pair combinations.



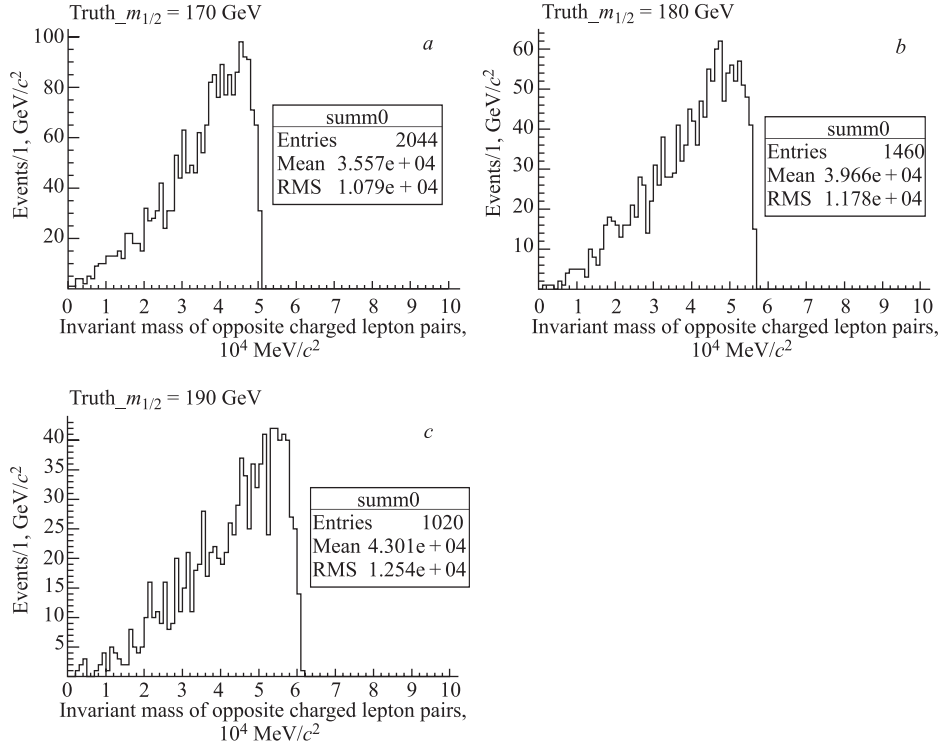


Fig. 8. Invariant mass distributions of the opposite-sign charged lepton pairs,  $m_{ll}$ , for the dilepton  $\tilde{g}\tilde{g}$ -pair decay channel generated at the parton level with different  $m_{1/2}$

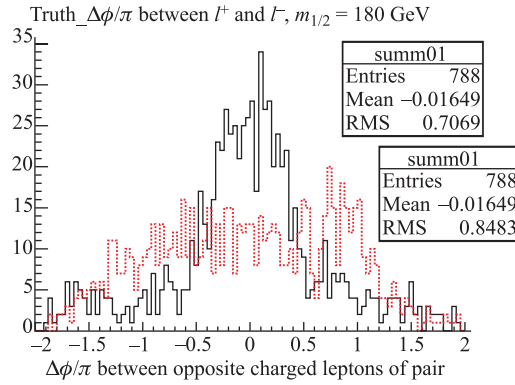


Fig. 9. Distributions of «truth» (solid) and «false» (dashed) combinations of opposite-sign charged leptons in the pair. Here  $\Delta = \phi_1 - \phi_2$  and  $\phi_1, \phi_2$  are the azimuth angles of the leptons in the pair. It is seen that the «truth» combinations are, in general, closer to zero than the «false» combinations. The former has the Root Mean Square (RMS) = 0.7069, but the latter RMS = 0.8483

To reconstruct the right signature and to choose the «truth» combinations of the lepton pairs, we have required four  $b$  jets and two opposite-sign charged lepton pairs in the event.

These selection criteria cut significant part of events, mainly due to the requirement of four  $b$  jets. All cuts passed only about 7% of all generated events. The distributions of the OS lepton pairs are shown in Fig. 10.

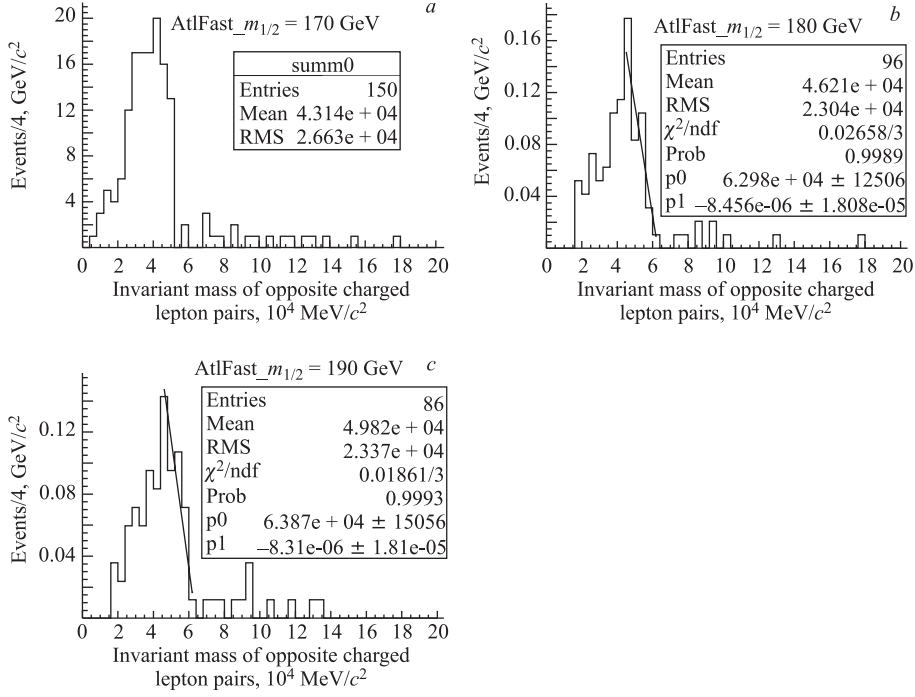


Fig. 10. Reconstructed invariant masses of the opposite-sign charged lepton pairs in the dilepton  $\tilde{g}\tilde{g}$ -pair decay channel

One can see that some events in the distributions have endpoint values of reconstructed dilepton masses  $m_{ll}$  larger than  $m_{ll}^{\text{expected}}$  (see Table 2) for the relevant  $m_{1/2}$ ; i.e.,  $m_{ll} > m_{ll}^{\text{expected}}$ . This was partly due to the inevitable contribution of the «false» combinations of the OS lepton pairs.

To extract the endpoint values, the fitting of the right slope of the obtained distribution was carried out with the function:

$$f_1(m_{ll}) = p_1(m_{ll} - p_0), \quad (6)$$

where  $p_0$  shows the endpoint value of the slope. As one can see from Fig. 10, the errors in determination of the endpoint values  $p_0$  are about 25%. Therefore, using only the dilepton channel data looks insufficient to separate SUSY subpoints with this endpoint determination procedure.

**1.2. Endpoint Criteria with Lepton + Jets Decay Channel.** To improve the accuracy of the endpoint procedure, the lepton + jets  $\tilde{g}\tilde{g}$ -pair decay channel was included into consideration. As one can see from relations (3) and (4), in this channel instead of one of the two OS lepton pairs one has the quark–antiquark pair in the final state. Furthermore, the cross section

of the lepton + jets channel is about 20 times larger than the cross section of the dilepton channel (see Table 2). The relevant number of expected events per 3 years of LHC running at the high luminosity are given in Table 2. There is only one pair of the opposite-sign charged leptons in this kind of events, and the selection criteria for extraction of such events are similar to the dilepton channel with corresponding changes.

Moreover, besides the linear fit of distributions used for dilepton channel (see Fig. 10), in this case an alternative method for cross-checking of the endpoint parameter determination based on data fitting with double Gauss function was included. The function [20]

$$f_2(m_{ll}) = \begin{cases} p_0 \exp(0.5((m_{ll} - p_1)/p_2)^2), & m_{ll} < p_1, \\ p_0 \exp(0.5((m_{ll} - p_1)/p_3)^2), & m_{ll} > p_1 \end{cases} \quad (7)$$

was used to fit right and left slopes of the  $m_{ll}$  distributions. The function has common mean ( $p_1$  parameter) and maximum ( $p_0$  parameter) values, but different «left» and «right» dispersions ( $p_2$  and  $p_3$  parameters). The value of wanted endpoint in this case equals sum of mean-value ( $p_1$  parameter) of  $f_2(m_{ll})$  and half-width,  $2.34p_3/2$ . We expect that the

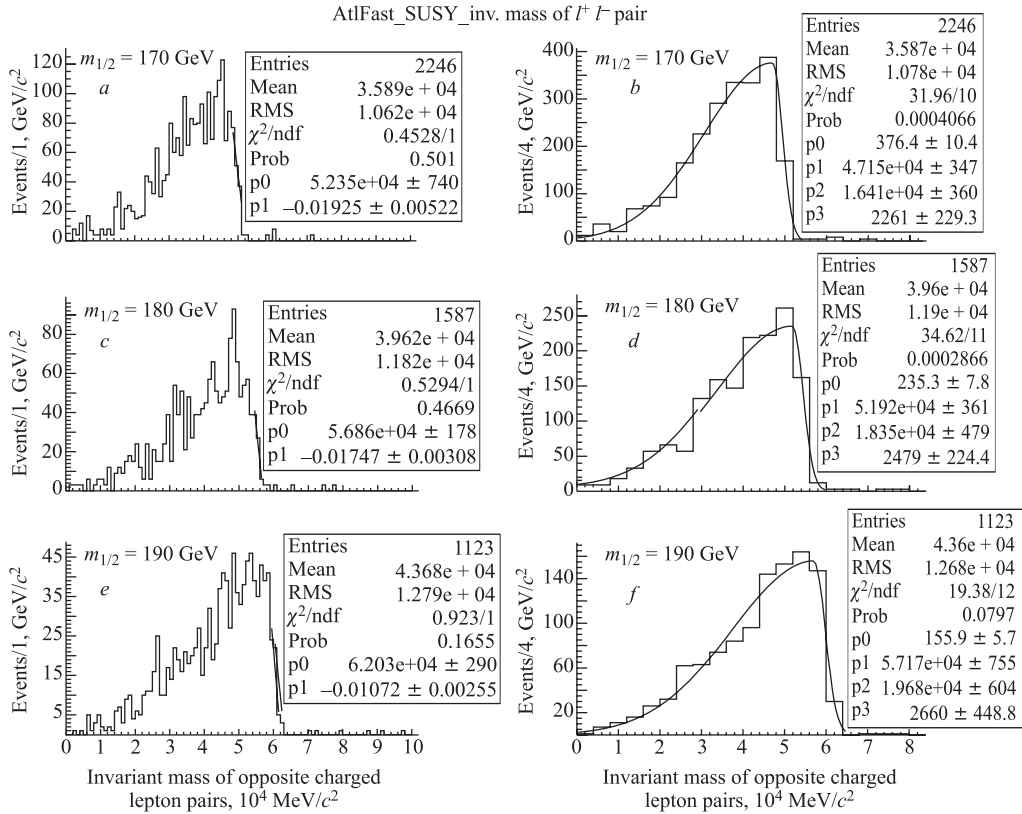


Fig. 11. Reconstructed invariant masses of opposite charged lepton pairs in both dilepton and lepton + jets  $\tilde{g}\tilde{g}$ -pair decay channels. Fit by linear function,  $f_1(m_{ll})$ , is given in Figs. a, c, e and fit by Gaussian function,  $f_2(m_{ll})$ , is given in Figs. b, d, f

extracted endpoint value with Gaussian fit function  $f_2(m_{ll})$  will be a bit less than with linear fit function  $f_1(m_{ll})$ , but anyway it is an estimate of the theoretically expected value  $m_{ll}^{\text{expected}}$  (see Eq. (5)). Figure 11 shows distributions of lepton-pair invariant masses,  $m_{ll}$ , reconstructed from dilepton and lepton+jets  $\tilde{g}\tilde{g}$ -pair decay channels.

These distributions are fitted by the linear function  $f_1(m_{ll})$  and the Gaussian function  $f_2(m_{ll})$ . The final results of both these fitting procedures are collected in Table 3. It is seen

**Table 3. Obtained endpoint results of the linear and Gaussian fits of the dilepton and lepton + jets channels (see Fig. 11) together with expected endpoint values (from Table 2)**

Subpoints	Endpoint values, GeV		
	Linear fit	Gaussian fit	Expected ( $m_{\tilde{\chi}_2^0} - m_{\tilde{\chi}_1^0}$ )
$m_{1/2} = 170$ GeV	$52.35 \pm 0.76$	$49.40 \pm 0.44$	50.9
$m_{1/2} = 180$ GeV	$56.86 \pm 0.18$	$54.40 \pm 0.57$	57
$m_{1/2} = 190$ GeV	$62.03 \pm 0.29$	$59.83 \pm 1.05$	61.09

from this table that both fitting methods allow the considered SUSY EGRET subpoints to be distinguished with more than  $5\sigma$  confidence level calculated with the equation

$$n(\text{C.L.}) = \frac{|m_1 - m_2|}{\sqrt{(\delta m_1)^2 + (\delta m_2)^2}}, \quad (8)$$

where  $m_{1,2}$  and  $\delta m_{1,2}$  are the obtained values of the endpoints and their errors, respectively.

To obtain this result, one has at least to investigate the reconstructed invariant mass distributions of opposite charged lepton pairs in both dilepton and lepton + jets  $\tilde{g}\tilde{g}$ -pair decay channels at  $300 \text{ fb}^{-1}$  statistics of the LHC.

## 2. STUDIES OF SOME BACKGROUND PROCESSES

The signature of our main process for search for the gluinos (2) is the very peculiar. To single out it from any other process, one has to clear reconstruct from the data four  $b$  jets, two opposite-charged (lepton, or quark) pairs and rather high missing of the transverse momentum.

Nevertheless, there are some mimic Standard Model (SM) background processes (without any sparticles) with alike signature, for instance, with top quarks and gluons:

$$\begin{array}{ccccccc}
 pp(gg) \rightarrow gg(q\bar{q}) \rightarrow t & \bar{t} & t & \bar{t} & & & \\
 & \downarrow & \downarrow & & & & \\
 & b & \bar{b} + W^- (\rightarrow l^- + \nu_\mu) & & & & \\
 & & + W^+ (\rightarrow l^+ + \bar{\nu}_\mu). & & & & 
 \end{array} \quad (9)$$

Indeed, this process again has four  $b$  quarks (four  $b$  jets), two OS lepton pairs and the missing transverse momentum, but from two neutrinos. The cross section of the processes  $gg(q\bar{q}) \rightarrow t\bar{t}t\bar{t}$  equals 2.67 fb (Acer MC-generator and with CTEQ5L PDF set was used) [11–17]. Therefore, at the total LHC luminosity of  $10^{34} \cdot \text{cm}^{-2}\text{s}^{-1}$  the expected rate of  $gg, q\bar{q} \rightarrow t\bar{t}t\bar{t}$  (or  $W^+bW^-\bar{b}W^+bW^-\bar{b}$ ) is up to 267 events per year at high luminosity. The requirement that

all of the four  $W$  bosons decay into the lepton–neutrino pair (with  $\text{BR}(W^- \rightarrow l^- \nu_l) \approx 0.1082$ ,  $l = e$  or  $\mu$ ), which is needed to reach the same signature as one for the SUSY process (2), reduces the rate of the SM background process (9) to about 0.5 events per three years at high LHC luminosity.

Another potential SM background process is the associative SM Higgs boson and top–antitop quark pair production  $gg(q\bar{q}) \rightarrow t\bar{t}H$  with subsequent Higgs boson decay into  $b\bar{b}$  pair ( $H \rightarrow b\bar{b}$ ). In this case, one has at least four  $b$  jets in the final state — the main SUSY-like signature in question — together with lepton–neutrino pair or/and some light-jets. The cross sections of these SM background processes and the expected number of events at the LHC both depend on the SM Higgs boson mass  $m_H$  only. In fact, the cross sections decrease very quickly with  $m_H$  increases [21].

The cross sections, branching ratios and expected number of events per three years of LHC running at high luminosity for  $gg(q\bar{q}) \rightarrow t\bar{t}\bar{t}\bar{t}$ ,  $gg(q\bar{q}) \rightarrow t\bar{t}H \rightarrow b\bar{b}t\bar{t}$ , and some other SM background processes are shown in Table 4.

**Table 4. Cross section and number of events for some SM backgrounds expected after 3 years of LHC running at high luminosity ( $300 \text{ fb}^{-1}$ ). The Alpgen MC generator with PDF = CTEQ6L [10,18] was used for the first three processes and PYTHIA was used for the last four [21]. The process  $pp \rightarrow 4b + 4\text{jets} + X$  has no any missing energy**

Background process	$\sigma \cdot \text{Br}$ , fb	Events
$pp \rightarrow t\bar{t}t\bar{t} \rightarrow (2b\bar{b} + 2l^+l^- + 2\nu\bar{\nu})$	$5.2 \cdot 0.0006$	0.936
$pp \rightarrow ZQQ + \text{jets} \rightarrow (l^+l^- t\bar{t}(\rightarrow bbl^+l^- \nu\bar{\nu})bb)$	$6.7 \cdot 0.001344$	2.7
$pp \rightarrow ZZZZ \rightarrow (2l^+l^- + 2b\bar{b})$	$3 \cdot 10^{-5}$	0.009
$pp \rightarrow 4b + 4\text{jets} + X$ ( $m_H = 200 \text{ GeV}/c^2$ )	0.2	60
$pp \rightarrow 4b + 4\text{jets} + X$ ( $m_H = 300 \text{ GeV}/c^2$ )	$10^{-3}$	0.3
$pp \rightarrow 4b + 2\text{jets} + \nu\mu + X$ ( $m_H = 200 \text{ GeV}/c^2$ )	0.02	6
$pp \rightarrow 4b + 2\text{jets} + \nu\mu + X$ ( $m_H = 300 \text{ GeV}/c^2$ )	$10^{-4}$	0.03

Therefore, our preliminary estimations of the SM background reveal its negligible contribution in the expected total number of signal events. Moreover, due to the masslessness of neutrinos the missing transverse momentum is expected to be much smaller than in the SUSY processes (2). This feature provides a possibility to distinguish between the background processes (9) and others in Table 4 and the SUSY process (2) by choosing the events with the large missing transverse energy (for instance, larger than 50 GeV).

Despite this optimistic situation, we plan to preform special investigation of all possible sources of any background processes which can mimic our specific SUSY-like signatures (namely, four  $b$  jets, two opposite-charged (lepton, or quark) pairs and rather high missing of the transverse momentum).

## CONCLUSION

To conclude, the prospects for ATLAS observation of a SUSY-like signal from two gluinos are under investigation. The region of the mSUGRA relevant to SUSY dark matter interpretation of the EGRET observation is considered. The cross section of the two gluinos

production via gluon–gluon fusion,  $gg \rightarrow \tilde{g}\tilde{g}$ , is rather high in the region. Studies of some SM backgrounds show that these processes did not make any significant contribution to signal. The clear signatures of chosen processes give ability to extract our EGRET point and even to distinguish subpoint with different  $m_{1/2}$  parameters from each other at more than  $5\sigma$  confidence level. Figure 12 shows confidence levels that could be achieved for distinguishing subpoints at different integrated luminosity.

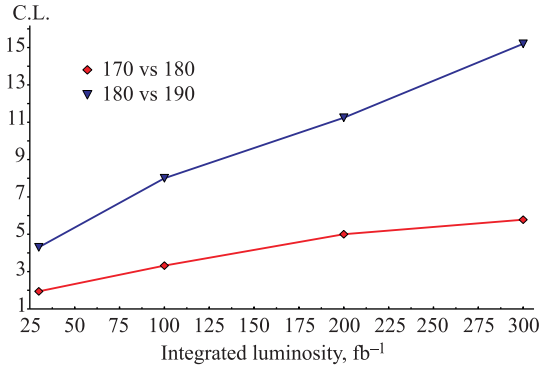


Fig. 12. Expected confidence level of distinguishing  $m_{1/2}$ -parameter subpoints at different integrated LHC luminosity

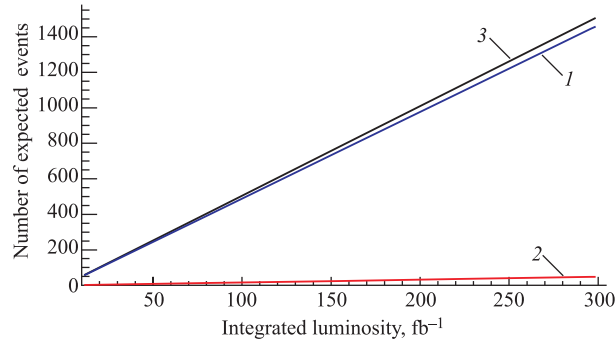


Fig. 13. Number of expected «lepton + jets» (1), «dilepton» (2) and their sum (3) events at the different integrated LHC luminosity with  $m_{1/2} = 180$  GeV

Moreover, the systematic errors from different PDF models (see Table 1 could also be estimated if one assumes that only cross section (and as a consequence the number of events) depends on the PDF model. For example, the cross section with PDF model CTEQ6L1 is 1.65 times smaller than with MRST\_2004\_nnlo and the expected confidence levels for these models of distinguishing SUSY subpoints at the same integrated luminosity ( $100 \text{ fb}^{-1}$ , for example) can be estimated from Fig. 12. Indeed the confidence level for CTEQ6L1 model corresponds to integrated luminosity  $100 \text{ fb}^{-1}$ , while the confidence level for MRST\_2004\_nnlo model corresponds to integrated luminosity  $165 \text{ fb}^{-1}$ .

The obtained results allow us to estimate number of expected events after selection criteria (see Sec. 1) as a function of integrated luminosity for «dilepton», «lepton + jets» and their

sum events for subpoint with  $m_{1/2} = 180$  GeV (see Fig. 13). It was done in the assumption that overall efficiency of selection criteria does not depend on luminosity of LHC the using the following equation:

$$N_{\text{expected}} = \alpha \sigma_{\text{signal}} L_{\text{integrated}}, \quad (10)$$

where  $\alpha$  is the ratio of number of events after selection criteria to number of events before selection criteria (equal to 0.066, 0.12 and 0.117 for «dilepton», «lepton + jets» and their sum, respectively),  $\sigma_{\text{signal}}$  is the cross section of the decay channel (equal to 2.435, 40.7 and 43.135 fb for «dilepton», «lepton + jets» and their sum, respectively), and  $L_{\text{integr}}$  is the integrated luminosity of the LHC (varied from 10 to 300 fb<sup>-1</sup>).

In particular, already at the LHC integrated luminosity 100 fb<sup>-1</sup> one can expect to see the SUSY-like signal of the EGRET gluinos by means of about 500 signal events in the lepton-jets decay channels of these gluinos.

**Acknowledgements.** Financial support from the Russian Foundation for Basic Research (grants #05-02-17603, #06-02-04003), the grant of the President of the Russian Federation for support of leading scientific schools (NSh-5362.2006.2) and ISTC grant G-1458 are kindly acknowledged.

#### REFERENCES

1. *Nilles H. P.* // Phys. Rep. 1984. V. 110. P. 1;  
*Haber H. E., Kane G. L.* // Phys. Rep. 1985. V. 117. P. 75;  
*Haber H. E.* Introductory Low-Energy Supersymmetry. Lectures given at TASI 1992. SCIPP 92/33. 1993; hep-ph/9306207;  
*Kazakov D. I.* Beyond the Standard Model: in Search of Supersymmetry. Lectures at the Eur. School of High-Energy Physics. 2000. hep-ph/0012288;  
*Kazakov D. I.* Beyond the Standard Model. Lectures at the Eur. School of High-Energy Physics. 2004. hep-ph/0411064.
2. *Bennett C. L. et al.* // Astrophys. J. Suppl. 2003. V. 148. P. 1;  
*Spergel D. N. et al.* // Ibid. P. 175.
3. *Hartman R. C. et al.* (EGRET Collab.) // Astrophys. J. Suppl. 1999. V. 123. P. 70;  
EGRET public data archive. <ftp://coss.c.gsfc.nasa.gov/compton/data/egret/>
4. *Bernabei R. et al.* // Riv. Nuovo Cim. 2003. V. 26. P. 1.
5. *Bednyakov V. A., Klapdor-Kleingrothaus H. V.* // Phys. Rev. D. 2004. V. 70. P. 096006.
6. *Bogachev D. Y. et al.* // Intern. J. Mod. Phys. A. 2006. V. 21. P. 5221.
7. *Paige F. E. et al.* ISAJET 7.69: A Monte Carlo Event Generator for  $pp$ , anti- $pp$ , and  $e^+e^-$  Reactions. hep-ph/0312045.
8. *Sjostrand T. et al.* Pythia 6.3 Physics and Manual. FERMILAB-PUB-03-457, LU-TP-03-38. hep-ph/0308153.
9. *Bednyakov V. A. et al.* hep-ex/0608060.
10. *Pumplin J. et al.* // JHEP. 2002. 0207. 012.

11. *Lai H. L. et al.* // Eur. Phys. J. C. 2000. V. 12. P. 375–392.
12. *Martin A. D. et al.* // Eur. Phys. J. C. 2002. V. 23. P. 73–87.
13. *Martin A. D. et al.* // Phys. Lett. B. 2004. V. 604. P. 61–68.
14. *Giele W. T., Keller S. A., Kosower D. A.* Parton Distribution Function Uncertainties. hep-ph/0104052.
15. *Alekhin S. I.* // Eur. Phys. J. C. 2000. V. 12. P. 375–392.
16. *Botje M.* // Eur. Phys. J. C. 2000. V. 14. P. 285–297.
17. *Kersevan B. P., Richter-Was E.* The Monte Carlo Event Generator AcerMC Version 2.0 with Interfaces to PYTHIA 6.2 and HERWIG 6.5. TPJU-6-2004. hep-ph/0405247.
18. *Mangano M. L. et al.* // JHEP. 2003. 0307. 001.
19. *Gjelsten B. K., Miller D. J., Osland P.* // JHEP. 2004. 0412. 003.
20. *Boyko I. R.* Private Communication.
21. *Krasnoslobodtsev I. V.* Study of  $4b$ -Jet Process at the LHC. Diploma Thesis. Moscow State Univ., 2007.

Received on February 5, 2008.